Electronic Supplementary Material (ESI) for Physical Chemistry Chemical Physics.

Supporting Information

Nanoscale domain imaging of Li-rich disordered rocksalt-type cathode materials with X-ray spectroscopic ptychography

Hideshi Uematsu,* Nozomu Ishiguro,* Masaki Abe,
Shuntaro Takazawa, Jungmin Kang, Itsuki Konuma,
Naoaki Yabuuchi and Yukio Takahashi*

Sample synthesis

The samples were prepared as follows: Li_2CO_3 (98.5 %, Kanto Kagaku) and V_2O_3 (98 %, Sigma Aldrich Japan) were mixed by wet ball milling, pressed into pellets. Then, $LiVO_2$ was synthesized from the pellet calcined in argon atmosphere at 1173 K for 12 h. The $Li_{10/7}V_{6/7}O_2$ was synthesized with mixing stoichiometric amount of Li_2O (97%, Sigma Aldrich Japan) and the synthesized $LiVO_2$, were mixed by mechanical milling (MM) using a planetary ball mill (PULVERISETTE 7; FRITSCH) with a zirconia pot (45 mL) and balls for 36 hours in argon atmosphere at a rotation speed of 600 rpm. $LiVO_3$ was synthesized from a mixture of Li_2CO_3 (Kanto Kagaku) and V_2O_5 (Wako Chemical Co.). The mixture was pressed into a pellet. 3 mol% excess Li_2CO_3 was added to compensate for the vaporization of Li ions on heating, and then was calcined at 823 K for 2 h in air. $LiNiVO_4$ was synthesized from a mixture of Li_2CO_3 (Kanto Kagaku), $Ni(OH)_2$ (Wako Chemical Co.), and V_2O_5 (Wako Chemical Co.). 3 mol% excess Li_2CO_3 was added to compensate for the vaporization of Li ions on heating. The mixture was pressed into a pellet, and then was calcined at 1073 K for 12 h in air. Samples were stored in an argon-filled glovebox. Fig. S1 shows the X-ray diffraction patterns of $LiVO_2$ and Li_2O before and after MM, and as-prepared $Li_{10/7}V_{6/7}O_2$.

Electrochemical evaluation

As-prepared $Li_{10/7}V_{6/7}O_2$ by MM was mixed with acetylene black (HS-100, Denka, sample: acetylene black = 90: 10 in wt%) using a planetary ball mill at 300 rpm for 5 h. Thus, electrode performance of the carbon composite sample was evaluated. The slurry consisted of 76.5 wt% active material, 13.5 wt% acetylene black, and 10 wt% poly(vinylidene fluoride), was mixed and pasted on an aluminum foil used as current collector. The electrode was dried and heated at 120 °C in vacuum. Metallic lithium (Honjo Metal) was used as counter electrode. The electrolyte solution used was 1.0 $\mathrm{mol\ dm^{-3}}$ $LiPF_6$ dissolved in ethylene carbonate: dimethyl carbonate (1: 1 by volume) (Kishida Chemical, battery grade). A polyolefin microporous membrane was used as a separator. Two-electrode cells (TJ-AC, Tomcell Japan) were assembled in the argon-filled glovebox. Charge/discharge tests were conducted at a rate of 10 $\mathrm{mA\ h\ g^{-1}}$ at room temperature. Fig. S2 shows the charge/discharge curves of $Li_{10/7}V_{6/7}O_2$.

Conventional V *K*-edge XAFS spectroscopy

Conventional XAFS measurements were carried out using the BL37XU beamline of SPring-8 in the transmission geometry. The incident X-ray was monochromatized by a Si(111) double-crystal monochromator and Pt-coated mirrors. Pellets of as-prepared $Li_{10/7}V_{6/7}O_2$, delithieted $Li_{10/7}V_{6/7}O_2$, $LiVO_2$, and $LiNiVO_4$ powders diluted with boron nitride were used as samples. $LiVO_2$ and $LiNiVO_4$ are the standard compounds of octahedrally coordinated V^{3+} and tetrahedrally coordinated V^{5+}, respectively. Fig. S4 shows the V K-edge XAFS spectra of the pellet samples.

Evaluation of spatial resolution using phase retrieval transfer function

The spatial resolution of the images was evaluated using the phase retrieval transfer function (PRTF)[1]. PRTF is given as

$$\mathrm{PRTF}(q,E) = \frac{\langle \mathrm{FT}[T^{(rec)}(\mathbf{r}-\mathbf{r}_j,E)P^{(rec)}(\mathbf{r},E)]\rangle_{q_\theta,j}}{\langle\sqrt{I_j(\mathbf{q},\mathbf{E})}\rangle_{q_\theta,j}},$$

where $\mathbf{r_j}$ is scan center position at j-th scan, $T^{(rec)}(\mathbf{r},E)$ and $P^{(rec)}(\mathbf{r},E)$ are reconstructed object and probe functions, $I_j(\mathbf{q},E)$ is measured diffraction pattern at j-th scan, $\langle\cdot\rangle_{q_\theta}$ and $\langle\cdot\rangle_j$ are circular average of spacial frequency $\mathbf{q}$ and scan average, respectively. Full-period spatial resolutions of reconstructed images were estimated as cross point the line of $1/e$ in PRTF. The resolution was evaluated about the reconstructed images at the 5420 eV and 5540 eV (Fig. S5).

Supplementary figures and table

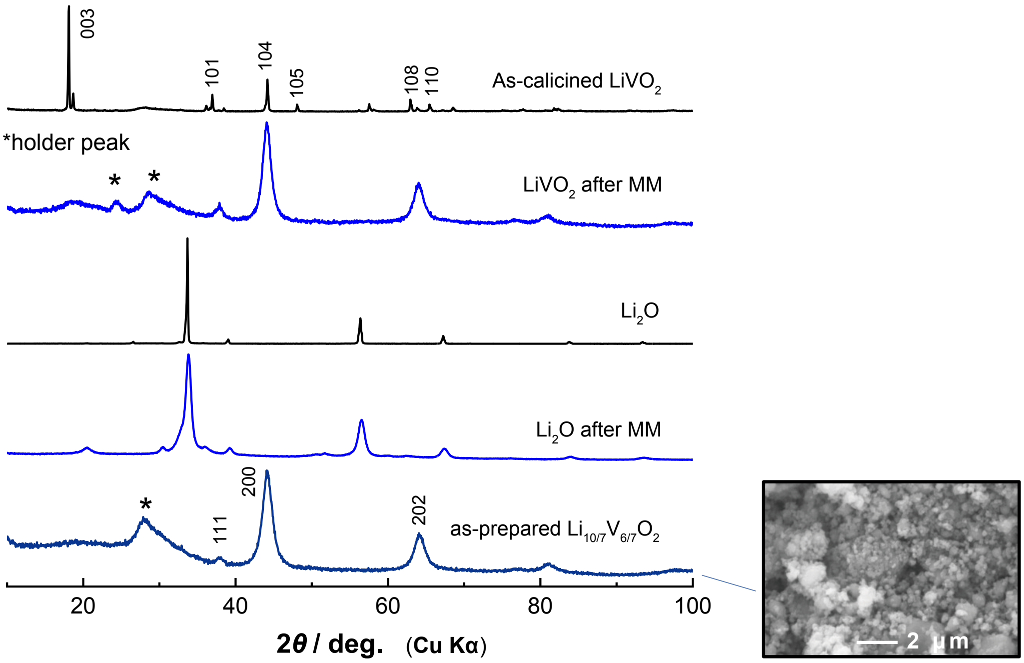

Fig. S1 X-ray diffraction patterns; $LiVO_2$ and Li_2O before and after mechanical milling (MM). The pattern of $Li_{10/7}V_{6/7}O_2$ obtained by MM from a mixture of Li_2O and $LiVO_2$ is also shown. The peaks of Li_2O disappear after MM with $LiVO_2$, suggesting solid solution formation and dissolution into $LiVO_2$ with the cation disordered rocksalt structure. Particle morphology of $Li_{10/7}V_{6/7}O_2$ observed by SEM is also shown.

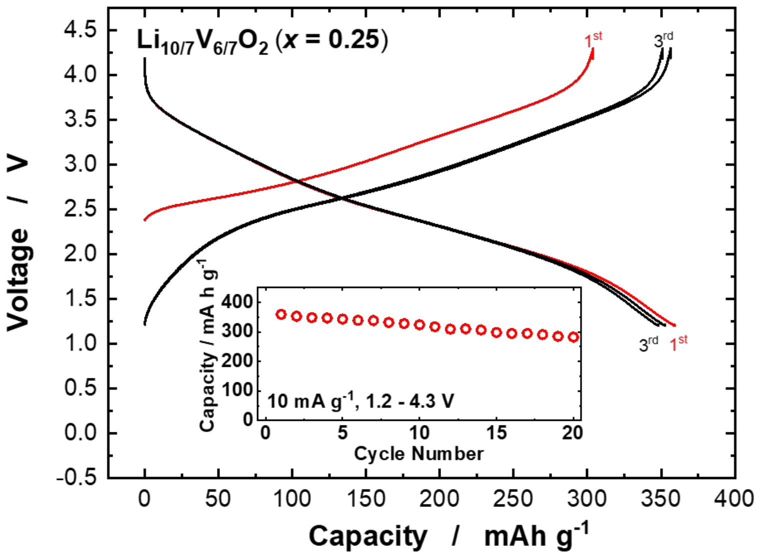

Fig. S2 Charge/discharge curves of $Li_{10/7}V_{6/7}O_2$ in a Li cell. Discharge capacity retention is also shown in the inset.

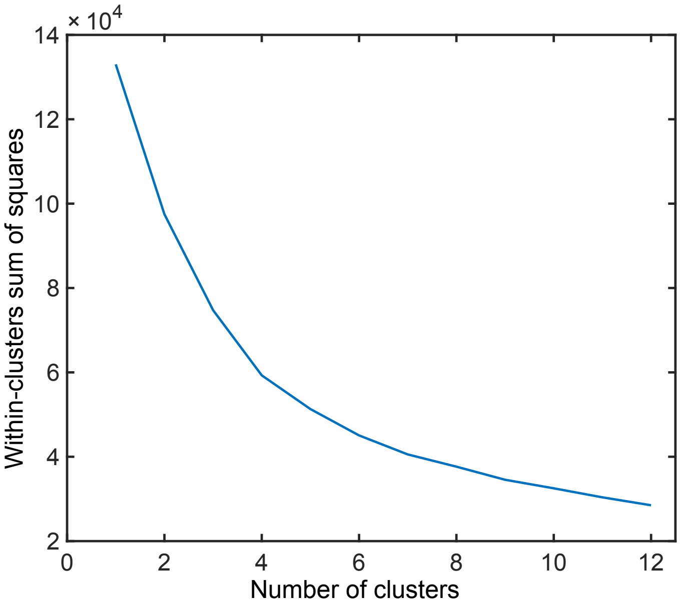

Fig. S3 Within-cluster sum of squared errors (SSE) vs. number of clusters k. We choose $k = 6$ as the number of cluster, because $k = 6$ onwards decrease flattens.

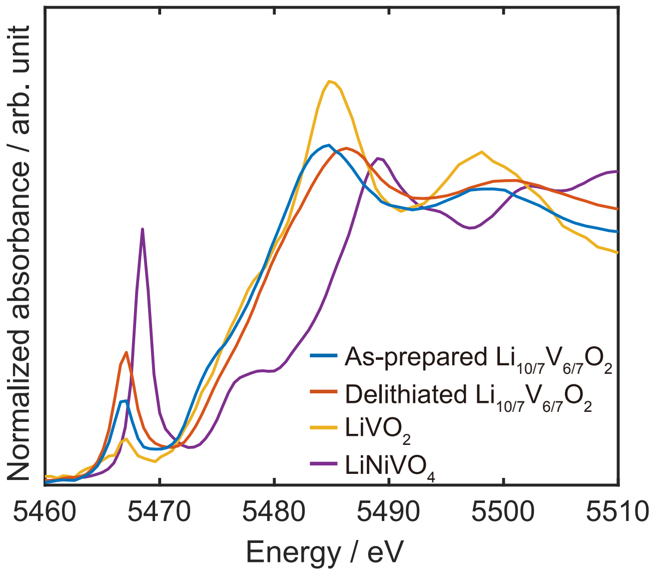

Fig. S4 Conventional V *K*-edge XAFS spectra of as-prepared $Li_{10/7}V_{6/7}O_2$, delithiated $Li_{10/7}V_{6/7}O_2$, $LiVO_2$, and $LiNiVO_4$ powders.

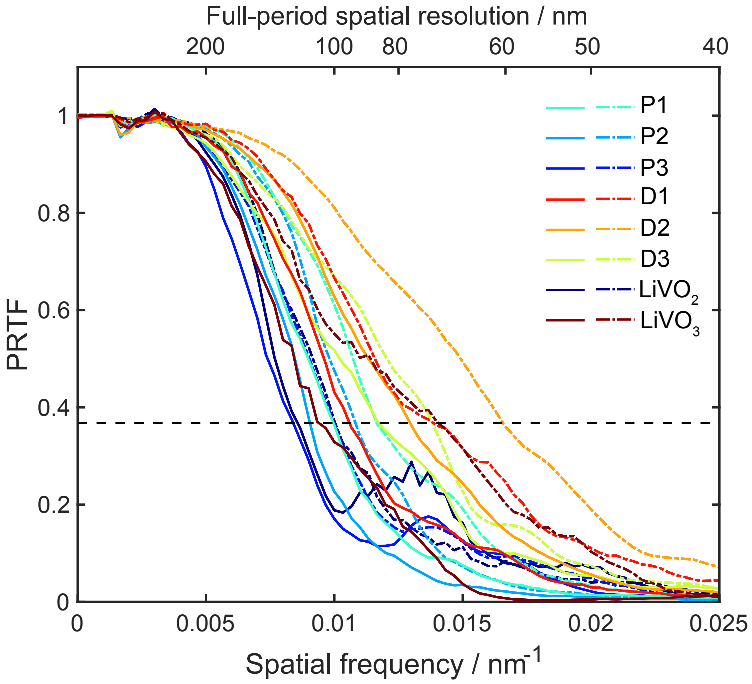

Fig. S5 Results of PRTF analysis of the reconstructed images of all particles measured by spectroscopic ptychography. The solid lines are at 5420 eV. The chain lines are at 5540 eV. The dashed line is $1/e$ threshold lines.

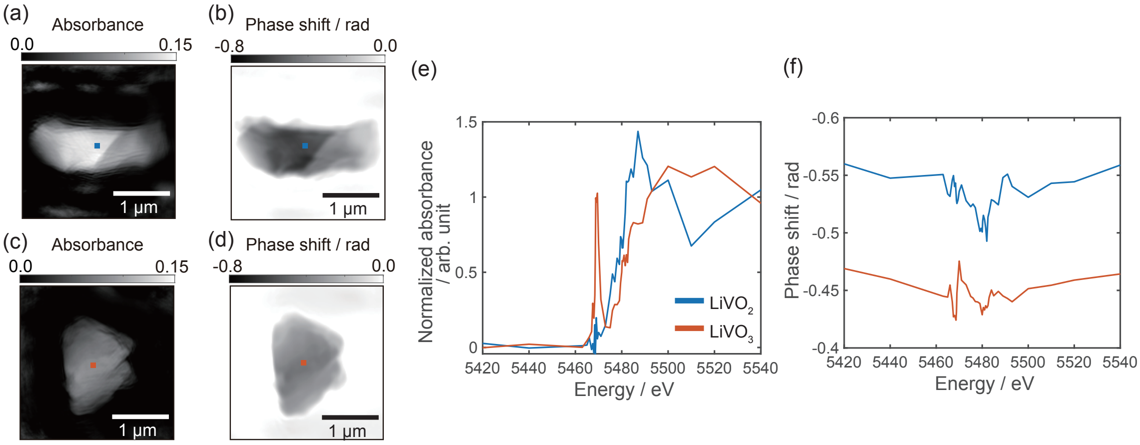

Fig. S6 Reconstructed images of (a) LiVO$_2$ and (b) LiVO$_3$. (left) reconstructed absorption images at 5540 eV and (right) phase shift images at 5420 eV in (a, b). The pixel size of recostructed images is 15 nm. (d) XANES (e) phase spectra of LiVO$_2$ and LiVO$_3$. The extracted size of the spectra (c and d) is $120 \times 120\ \mathrm{nm}^2$.

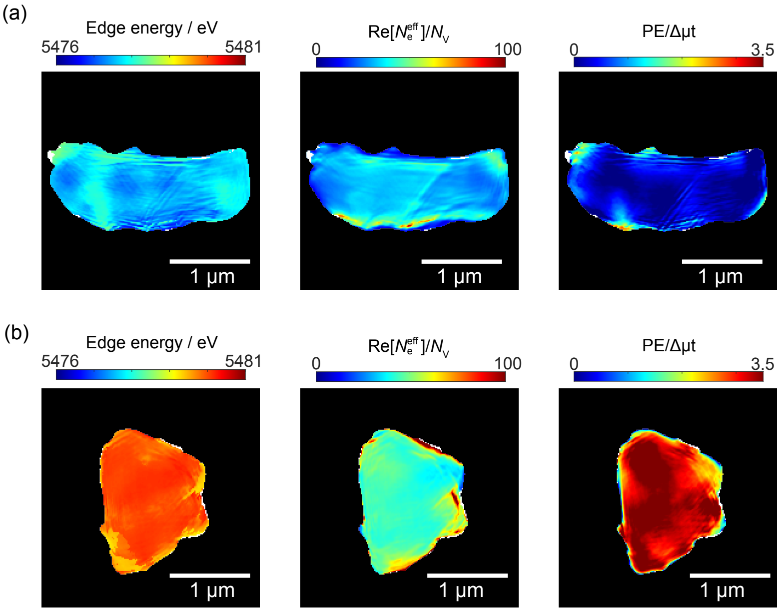

Fig. S7 Chemical state maps of (a) LiVO$_2$ and (b) LiVO$_3$. (left) Edge energy, (center) $\mathrm{Re}[N_{\mathrm{e}}^{\mathrm{eff}}]/N_{\mathrm{V}}$, and (right) $\mathrm{PE}/\Delta\mu t$ in (a,b).

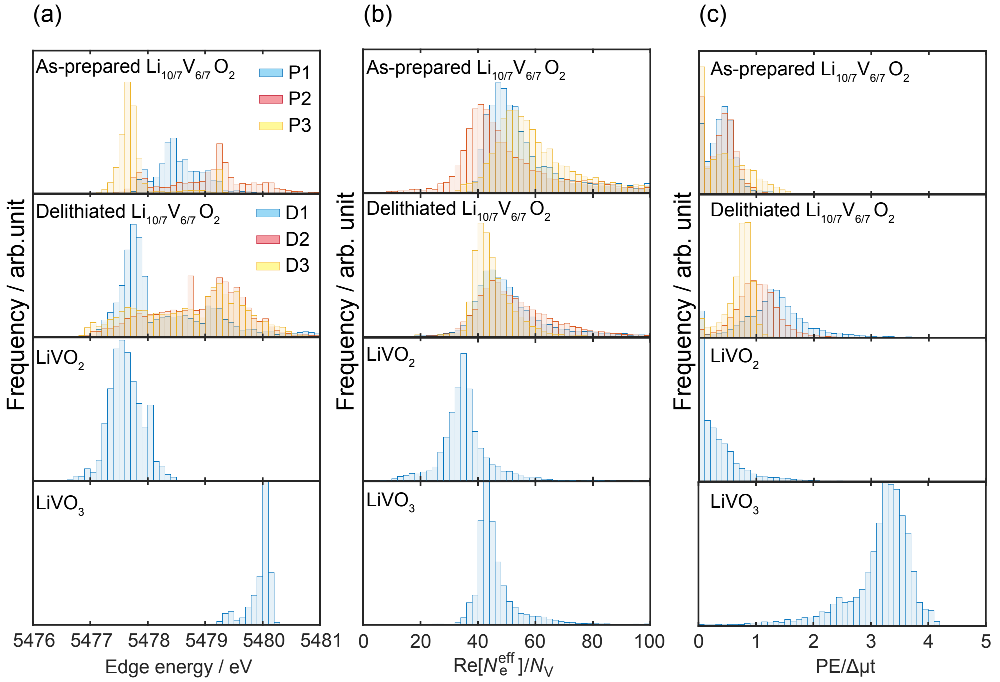

Fig. S8 Histograms of the chemical state in (a) edge energy (b) $\mathrm{Re}[N_\mathrm{e}^\mathrm{eff}]/N_\mathrm{V}$ (c) and $\mathrm{PE}/\Delta\mu t$, respectively.

Table 1 Average values of chemical states in each cluster

Cluster	Edge energy /eV	$\mathrm{Re}[N_e^\mathrm{eff}]/N_\mathrm{V}$ /e $\cdot$ atoms^{-1}	$\mathrm{PE}/\Delta\mu t$
1	5477.9	53.1	0.5
2	5477.9	53.8	1.4
3	5479.2	48.2	1.0
4	5479.7	50.2	0.4
5	5478.7	133.3	0.4
6	5477.9	102.3	2.9

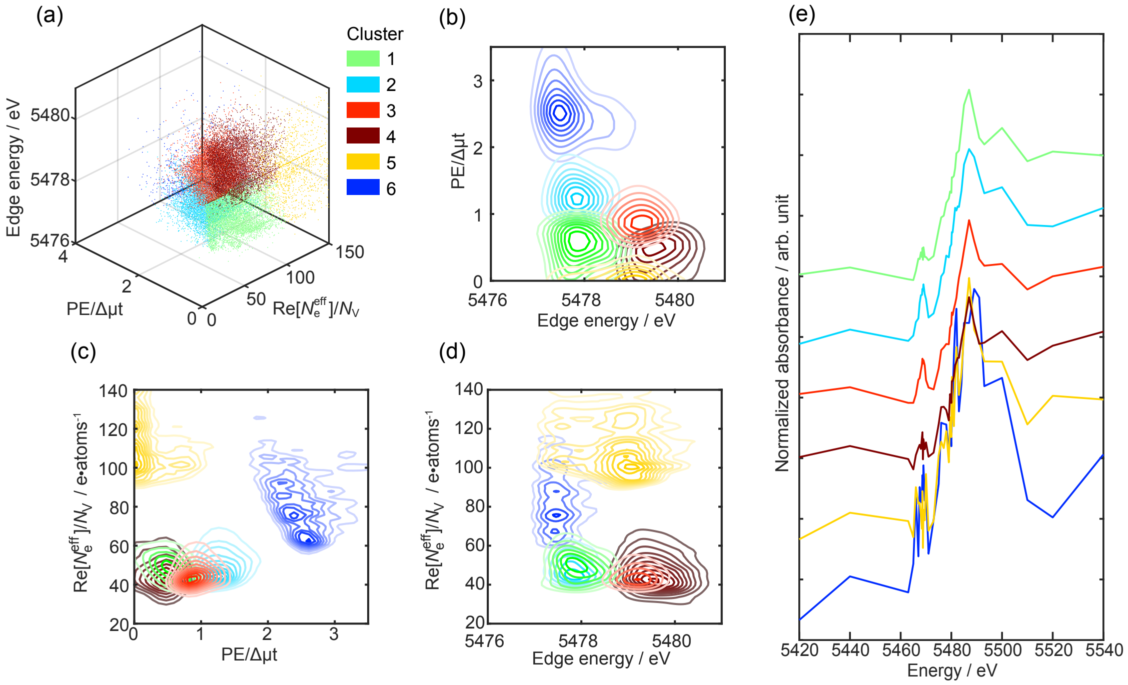

Fig. S9 (a) Three-dimensional scatter plot between edge energy, $\mathrm{Re}[N_\mathrm{e}^\mathrm{eff}]/N_\mathrm{V}$ and $\mathrm{PE}/\Delta\mu t$ for each cluster. (b-d) Two-dimensional projected probability density of each cluster. (b) $\mathrm{PE}/\Delta\mu t$ – Edge enegy (c) $\mathrm{Re}[N_\mathrm{e}^\mathrm{eff}]/N_\mathrm{V}$ – $\mathrm{PE}/\Delta\mu t$ and (d) edge energy – $\mathrm{Re}[N_\mathrm{e}^\mathrm{eff}]/N_\mathrm{V}$.(e) Average XANES spectra in each cluster.

Notes and references

1) H. N. Chapman, A. Barty, S. Marchesini, A. Noy, S. P. Hau-Riege, C. Cui, M. R. Howells, R. Rosen, H. He, J. C. H. Spence, U. Weierstall, T. Beetz, C. Jacobsen and D. Shapiro, *J. Opt. Soc. America A*, 2006, **23**, 1179.